ICIS EUROPEAN INTERNET CENTRE FOR IMPEDANCE SPECTROSCOPY

Impedance Contributions Online 4 (2006) P5-1 – P5-27
http://accessimpedance.iusi.bas.bg

CURRENT INTERRUPT TECHNIQUES AS A COMPLETION OF EIS: STRUGGLING AGAINST MUTUAL INDUCTION IN FUEL CELLS RESEARCH AND TIME SAVING IN BARRIER COATINGS CHARACTERIZATION

F. Richter[1], C.-A. Schiller [2*], W. Strunz [2], N. Wagner [3]

[1] *Siemens AG, KWU, Erlangen, Germany*
[2] *Zahner-elektrik, Kronach, Germany*
[3] *DLR, Stuttgart, Germany*
[*] *Corresponding author:* cas@zahner.de

ABSTRACT

Besides Electrochemical Impedance Spectroscopy (EIS), time-domain techniques can be applied successfully to supplement results of EIS for the development and improvement of particular commercially relevant products, in especially, considering 'both frequency limits' in very low or very high impedances.

Concerning low Ohmic systems like fuel cells, a basic limitation at high frequencies arises from the mutual induction effect. Using solely EIS, this effect may complicate the determination of Ohmic contributions within a fuel cell. To determine this important parameter accurately, the high current interrupt (HCI) technique can be used. As shown, HCI can extend the available frequency range about a factor of three to ten in a carefully optimized experimental set-up. Thus, an arrangement, which performs both, the standard EIS and the HCI measurement within one set-up, is the best choice for the challenges of electrochemical power source device testing.

Concerning high Ohmic systems like coating systems for corrosion protection, the big advantage of EIS is the rapid determination of the dielectric properties. But the determination of electrochemical parameters from impedance spectra may become cumbersome in the low frequency range because the duration of the measurement increases strongly. As an alternative in the time-domain, the Relaxation Voltammetry (RV) technique can supplement impedance measurements in the low frequency range. Furthermore, the RV equipment is less expensive so that several measurements can be performed in parallel, which reduces the time consumption in the manufacturer's laboratory additionally.

Keywords: impedance spectroscopy, time domain, fuel cells, high current interrupt, Z-HIT, relaxation voltammetry

1. INTRODUCTION

For the development and improvement of important and innovative commercial products like fuel cells or corrosion protective coatings, electrochemical investigations like Electrochemical Impedance Spectroscopy (EIS) became increasingly important within the last decade. Considering the time scale of involved, relevant processes, a significant advantage of EIS originates from the fact that this technique covers a range of at least 10 decades in the frequency domain.

In addition, the measured data can be evaluated and modeled easily by means of equivalent circuits. This means that the involved mathematical operations are formally pure algebraic ones in the frequency domain instead of solving differential equations in the time domain. This is even more convenient, in case the equivalent circuit has to be changed and therefore in the latter case a new differential equation has to be derived and solved accordingly. From these considerations it is not surprising that the application of EIS has become more and more dominant.

Judging by the experimental effort, the application of time-domain measurements is still attractive. Considering time- and frequency domain techniques, it is not a question, which type is more favourable or even supersedes the other technique. It is more a question, which one of the techniques is more suited to obtain access to a relevant parameter, considering the particular conditions this parameter has to be determined for.

As it will be shown in the following, time-domain techniques may supplement the results obtained from EIS.

2. HIGH CURRENT INTERRUPT (HCI) - MEASURING LOW IMPEDANCES AT HIGH FREQUENCIES

If a power generating device like a fuel cell is examined, its dynamic electrical equivalence generally will appear as a network, represented by the impedance contributions of anode, cathode, membrane, electrolyte and connectors.

The specific losses of every partial impedance of the network contribute to the overall efficiency of the device. The porous layers of anode and cathode, responsible for the charge transfer reaction, and the occurring mass transport normally play a major role. Other contributions seem to be less important. There is the resistance of the electrolyte or of the membrane as well as the resistance of contacts and connectors. A frequency-dependent part is added further by the inductance of the bulk and the connectors.

Nevertheless, the Ohmic part (electrolyte, membrane, connectors) plays an important role regarding the performance of the device and even dominates sometimes in the overall losses. In addition it is very sensitive to degradation caused by corrosion and thermal stress. In applications with dynamic load changes, for example in a laptop computer battery or in electromotive applications, the inductive parts are limiting the maximum pulse load available.

EIS in principle allows to separate all the characteristic contributions (Fig. 1). The Ohmic share can be determined simply in the high frequency region of a spectrum, where the impedance curve intersects the real axis (Fig. 2). The series inductance is expressed at successive higher frequencies in the diagram.

The experimental determination of the impedance requires several prerequisites. An important practical one is that measuring impedance always means to measure two signals synchronously: the current flowing through the system and the voltage across the system being tested.

The situation is sketched in Fig. 3 on the left hand side. Like any other measuring technique, the accuracy obtained in a practical application is limited by the presence of unwanted disturbances combined with the wanted information. This can be quantified by means of the signal-to-noise ratio. Fig.3 on the right hand side illustrates this by emphasizing the noise sources relevant to the situation measuring very low impedances, like it is the case with fuel cells or batteries.

The closer look at the circuit diagram shows that the voltage information may contain not only the interesting part present at the site of the connecting terminals. Dynamically induced voltages may contaminate the signals. These errors are caused by the unavoidable mutual induction from the magnetic field caused by the current flow. Mutual induction is a four-pole transfer function phenomenon and it should not be mixed with

duction is a four-pole transfer function phenomenon and it should not be mixed with self inductance or other two-pole impedance elements [1].

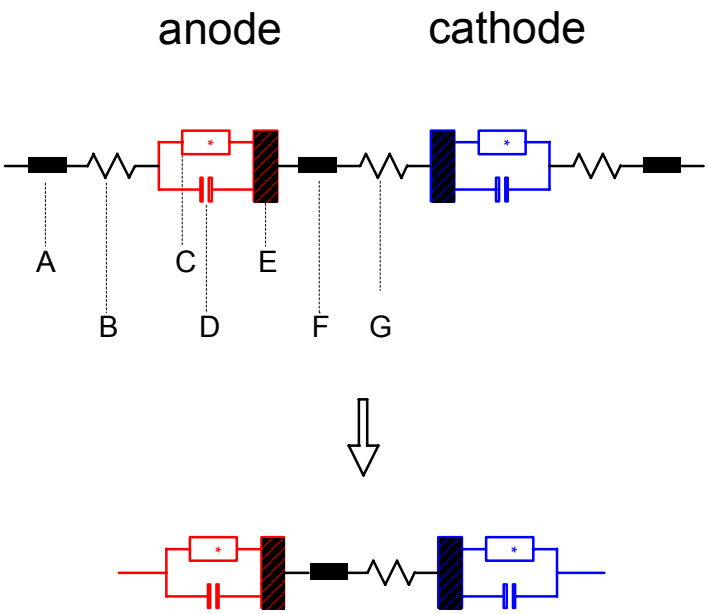


Fig. 1. Equivalent circuit of a fuel cell (upper part). A: connector inductivity, B: connector resistance, C: charge transfer (Faraday-) processes, D : double layer capacitance, E : porous distribution, F : bulk inductance, G : bulk (membrane, electrolyte) resistance. In the lower diagram the undistinguishable resistive and inductive contributions are grouped together.

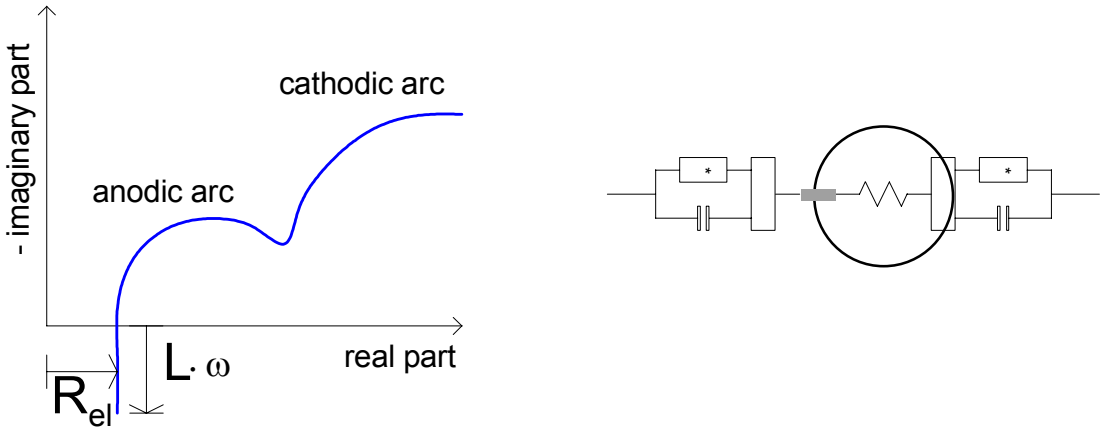


Fig. 2. The appearance of the Ohmic share R_{el} and the stray inductance L in a typical impedance spectrum of a fuel cell (left) and their location in the corresponding equivalent circuit (right).

This kind of interference increases with increasing frequency and with the transfer coupling efficiency of the magnetic field of the current in relation to the voltage drop across the sample. It depends strongly on the geometry and grows up with the dimensions of the object and it cannot be eliminated by calibration procedures [2]. This means for impedance investigation of power sources: the more you scale up, the lower is the available upper frequency limit f_g. At frequencies $f >> f_g$, the signal-to-noise ratio is too poor. Sufficient accuracy to determine the Ohmic share and the inductance can no longer be achieved.

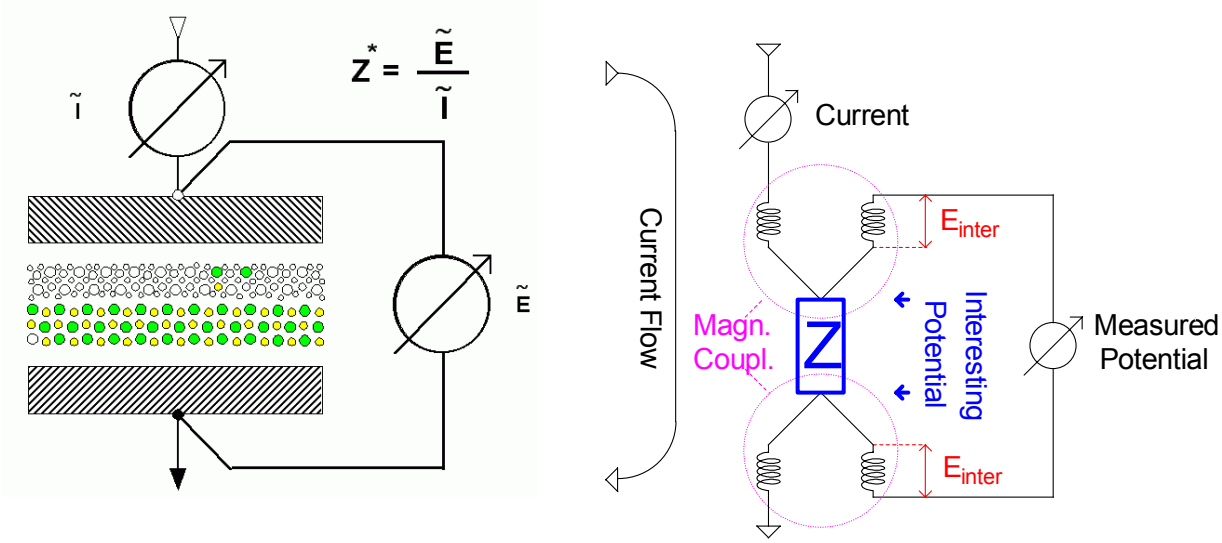


Fig. 3. Basic impedance measurement circuit – principle (left) and the details, how mutual inductance interferes with the potential value (right).

In practice there is a limit for the successful application of EIS to low Ohmic objects at high frequencies. As a rough estimate one can calculate the upper frequency limit $\mathbf{f_g}$ for these systems according to:

$$\mathbf{f_g} \approx 1\ \text{MHz} * |Z|_{min} / \Omega \qquad (1)$$

As a consequence, the window for obtaining relevant Ohmic resistance information by means of the EIS becomes smaller for larger cells. For certain systems, the window is closed.

What can be done to complement the EIS data under these conditions? The question is answered by the well known current interrupt technique, which does not require the acquisition of two signals simultaneously. The principle is shown in Fig. 4 and explained in the following:

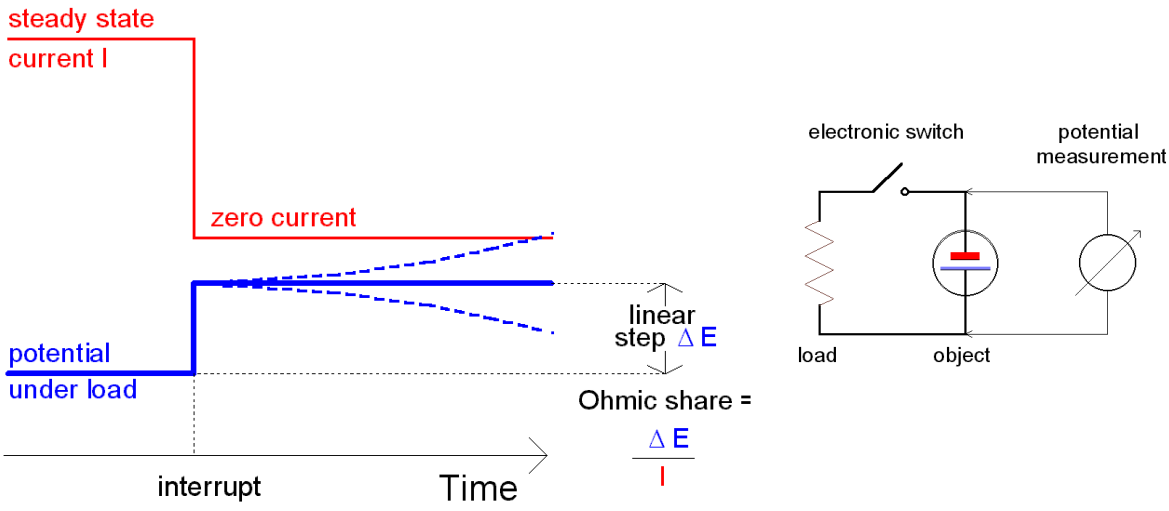


Fig. 4. The principle of the current interrupt technique. Signal course in the time domain (left) and the basic circuit (right).

A steady-state current *I* is interrupted by a switch. The step response of the potential *E* is sampled and analyzed, assuming that the current drops down instantaneously from its stationary value to zero.

In practice, the settling time depends on the electromagnetic energy stored in the parasitic capacitance and inductance of the cell and the instrumentation arrangement on the one hand and on the damping process on the other hand. Provided that the set-up is built up appropriately, the interruption results in a breakdown of the current to small values within a short time. In this case, the potential will be disturbed to a smallerextent by mutual induction than it is with an EIS measurement.

In theory, the Ohmic contribution to the overall impedance can easily be seen from the height of the fast rectangular step of the potential. For the evaluation a linear step model is commonly used.

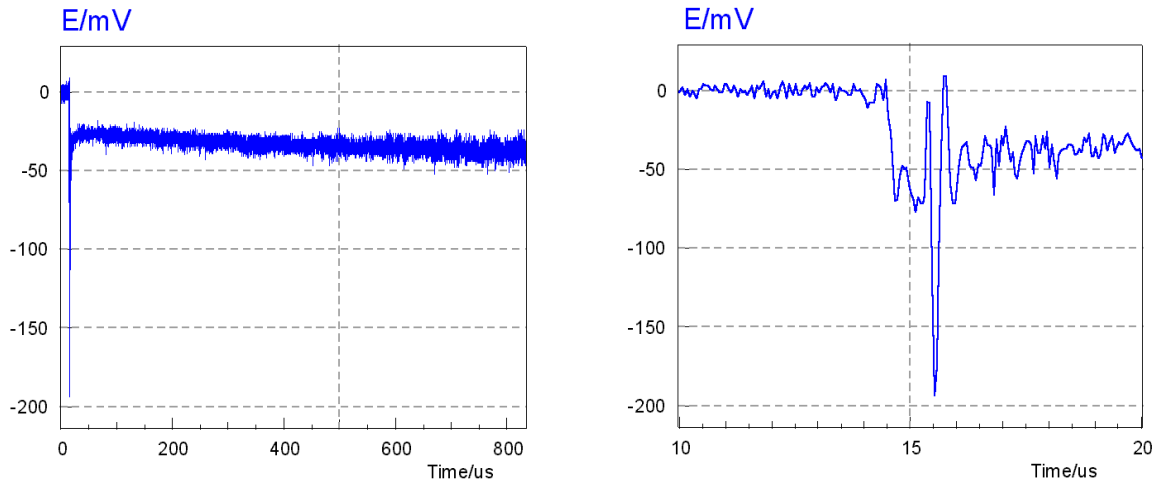


Fig. 5. Typical current interrupt potential step response. Long term (left) and short term (right) response of a single Polymer Electrolyte Membrane (PEM) fuel cell of area 23cm^2, at 80 °C and a current of 80 A.

But this evaluation suffers from the disadvantage that the analysis of the time domain data is interfered by the “ringing” in the signal as a result of the parasitic resonance. In addition, the early phase of the response is characterized by a non-linear behavior due to the imperfect characteristics of the electronic switch. Furthermore, the response of both double-layers of the cell may follow soon after the interruption, when the concentrations of the involved species change from their steady state values to new ones without load. All these effects bend and distort the expected ideal shape of the potential step. Therefore, the automatic analysis of pulse measurements by means of a simple fit to a linear step model often leads to inaccurate results.

The aim of the authors was to improve the method in order to obtained results of reliability comparable with that of EIS. The basic idea is not to evaluate the distorted step function in the time domain. Instead, after a transformation of the data into the frequency domain, the resulting spectrum and all parasitic effects can be analyzed by means of EIS methods.

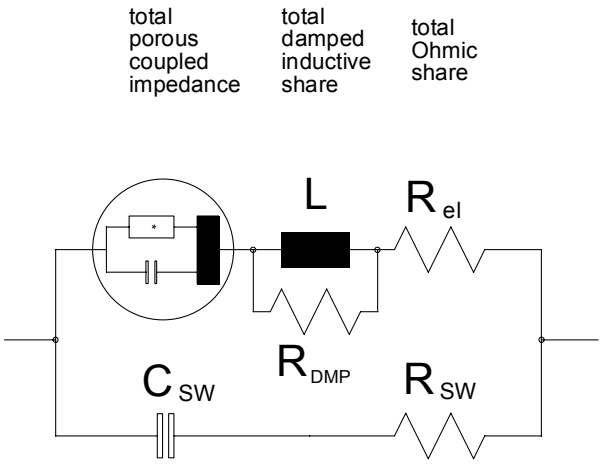


Fig. 6. Equivalent circuit for a high current interrupt (HCI) measurement set-up of an electrochemical power source device including the parasitic properties of the switching circuit.

In Fig. 6, a simplified equivalent circuit for a HCI measurement set-up of a power cell is shown. It contains the impedance of the active cell part (the circle), the integral inductance (L) and resistance (R) and the parasitic effects of the switching circuit. The resonance circuit is mainly built up of the series inductance, the double layer capacitance and the capacitance of the electronic switch. It is responsible for the overshot and "ringing" in the pulse response signal.

Fig. 7 illustrates the essential steps of the transformation of the time domain data into the frequency domain. The potential response signal E is sampled by a fast, high-resolution transient recorder. The numeric algorithms use discrete Fourier transform methods to achieve an effective analysis. In order to minimize the errors caused to their application on single events, a weighing function has to be applied. At least, a *Zoom FFT* calculates the amplitude spectrum in the frequency domain. A similar procedure was carried out before using a reference resistor for calibration. The quotient of both spectra finally leads to the modulus of the impedance of the unknown object.

This scalar impedance spectrum can be used to evaluate the Ohmic share in a simple, automated way. The user selects a reliable frequency range for the analysis, which excludes the parasitic resonance effects at the high frequency end. The impedance minimum within this range represents the Ohmic share with an accuracy of about ± 1 %.

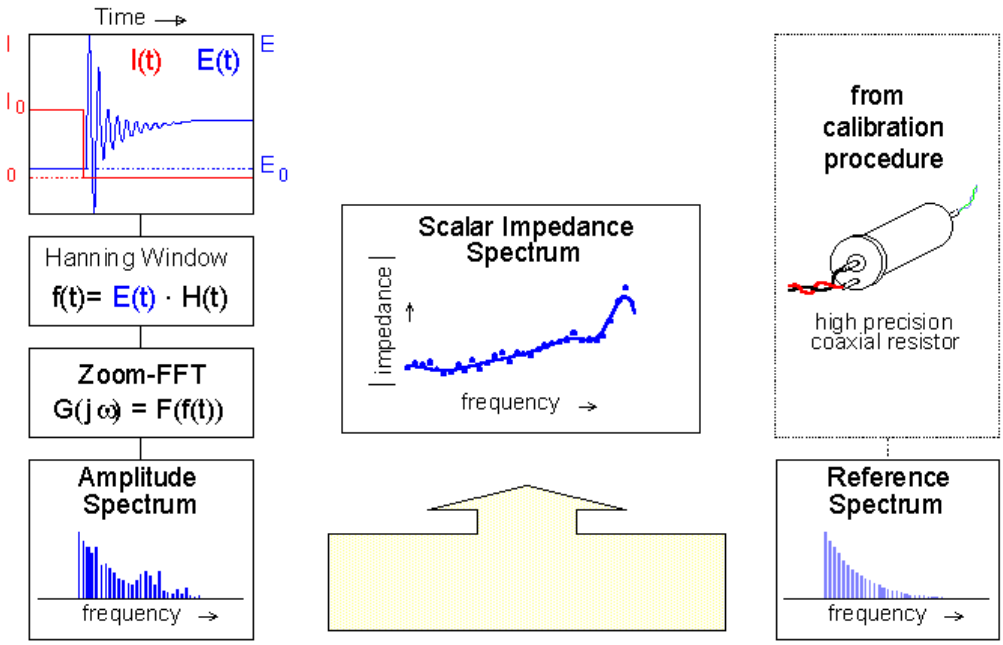


Fig. 7. The formal evaluation principle of HCI. The time domain data are transferred into the frequency domain. Dividing the spectrum by a reference spectrum leads to the scalar impedance spectrum of the object being tested.

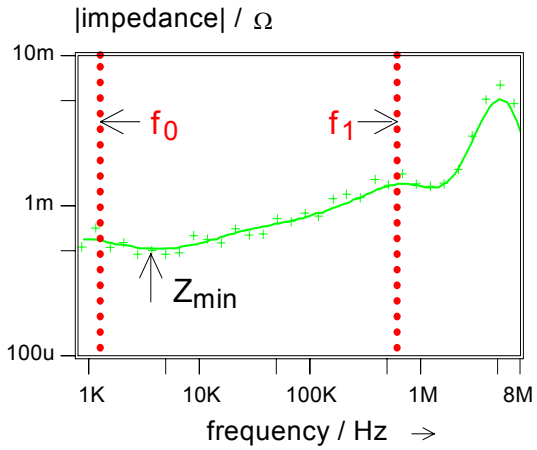


Fig. 8. Automatic evaluation of the Ohmic share from the minimum Z_{min} of the scalar impedance function.

If one wants to evaluate the response spectrum by the standard methods of EIS, beside the impedance, the phase data are necessary. For this calculation, a relationship between impedance and phase, which is valid for all two-pole impedance objects of minimum phase, can be used. The Z-HIT relation (eq. 2) allows to calculate approximately the

modulus of the impedance course from the change of the phase angle [3]. It will also be possible to perform the inverse application, if one uses the Z-HIT in an iterative numerical way. This is done by the HCI analysis software to obtain a complete spectrum (Fig. 9).

$$ln|H(\omega_0)| \approx \text{const.} + \frac{2}{\pi}\int_{\omega_S}^{\omega_0} \varphi(\omega)\, d\ ln\omega - \frac{\pi}{6}\cdot\frac{d\varphi(\omega_O)}{d\ ln\omega} \qquad (2)$$

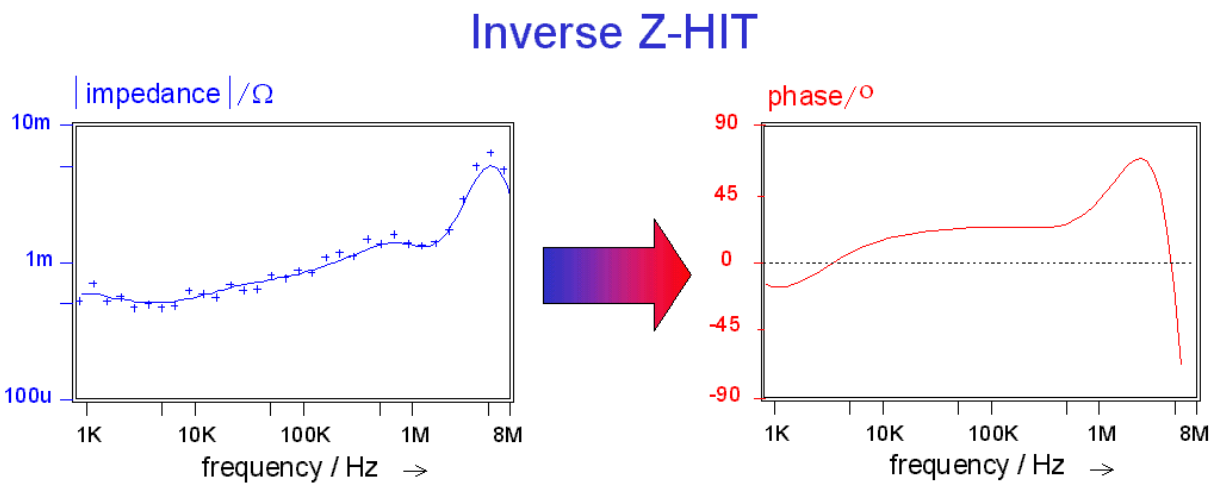


Fig. 9. Calculation of the phase angle from the impedance modulus by means of the inverse application of the Z-HIT transform. The Z-HIT equation (eq. 2) shows that the impedance modulus at the frequency ω_O can be calculated from the integral of the phase angle course $\varphi(\omega)$ within the limited frequency boundaries (ω_S(s=start) to ω_O). A correction term proportional to $d\varphi/d\ln\omega$ dramatically enhances the accuracy.

The complex spectrum can now be analyzed in the usual way, for instance, by means of simulation and fitting to an appropriate equivalent circuit. Based on the experience of the authors, the Ohmic share determined in this way can be detected with typically double or triple precision compared to simply relying on the minimum of the scalar impedance function.

Fig. 10 is a sketch of the practical set-up used for high current interrupt measurement of a fuel cell. The electrochemical cell (A) is connected to an electronic load (B) or another type of high power potentiostat to ensure steady state load conditions. Additionally, this potentiostat works as a fast electronic switch for the current interruption.

The potentiostat is controlled by an electrochemical workstation (D) including a fast, high resolution transient recorder. The recorder input is connected to the potential sensor lines of the cell through a so called *Pulse Probe* (C). The main task of the pulse probe is the galvanic isolation of the potential sensor circuit from the instrument in order to minimize the electromagnetic interference. On the other hand, it enables the protection of the instrument input by means of an energy consuming clipping circuit.

After a short 'sampling shot' during the interrupt, the instrument switches on the current again, in order to reestablish the steady state and to avoid a possible damage of the cell. The pulse response is analyzed then by the software of the workstation as described above.

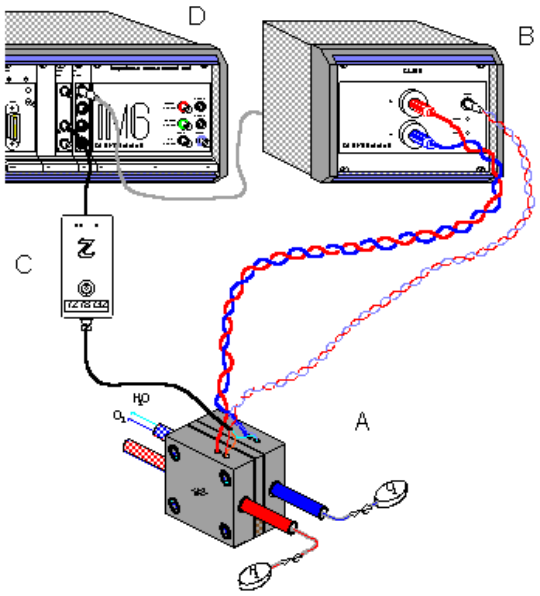


Fig. 10. Practical set-up of a high current interrupt fuel cell measurement

A series of test experiments have been done under controlled conditions. Compared with the standard EIS, the major experience is that the HCI is significantly less sensitive to artifacts caused by mutual induction. This is illustrated by the example depicted in Fig. 11. Here test measurements were performed with resistors using two different, intentionally non-optimized connection geometries. As one can see, the strong in-phase mutual induction of the above example simulates an inductive component, which ap-

pears unrealistically high in the case of the standard EIS. The HCI method, however, leads to an almost exact value.

For the other example, which has been omitted here shows a strong out-of-phase mutual induction, one obtains almost the same impedance functions. Yet, the phase diagram shows paradox behavior for the standard EIS curve. The course erroneously indicates capacitive characteristics! The phase curve of the HCI experiment shows the correct sign due to its origin from the Z-HIT transform.

It was also found, that the HCI experiment worked correctly with power generating devices. As an example, the results of an EIS and a HCI experiment at a high temperature fuel cell are depicted in Fig. 12. The cell has been driven with air and humidified hydrogen and generated more than four Amperes at a potential exceeding 0.73 Volts. In both experiments the best case wiring was used to reduce the mutual induction interference.

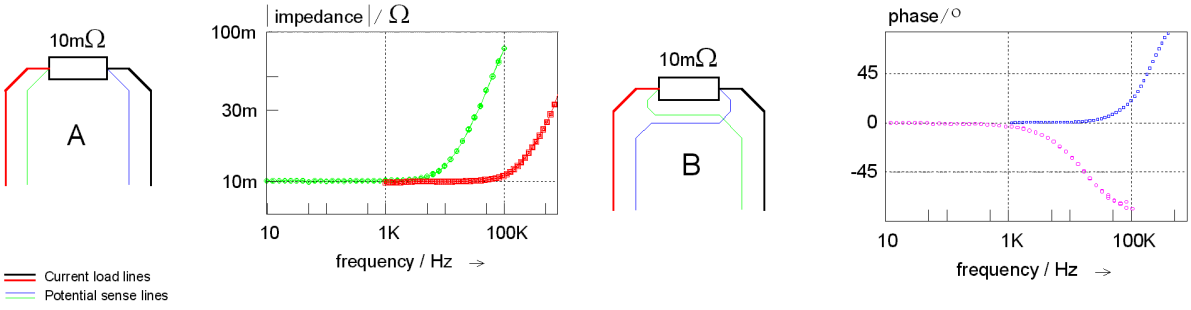


Fig. 11. Results of test measurements with reference resistors including mutual induction (MI) components. A: In phase MI leads to a high inductive response in the case of EIS (full dots) whereas the HCI spectrum (squares) matches the theory. B: Out-of-phase MI causes incorrect negative (capacitive) EIS phase courses (blue squares), while the HCI phase course shows the correct positive phase sign for inductance.

The original HCI potential step response is plotted on the left hand side of Fig. 12. At the right hand side, the transformed impedance (circles) as well as a comparative impedance measurement (rhombs) are drawn. As one can see, the methods complement one another ideally for the different frequency ranges. In this special case, the frequency

limit for the EIS experiment was high enough to achieve accurate information about the Ohmic share. Therefore, both methods give the same correct results.

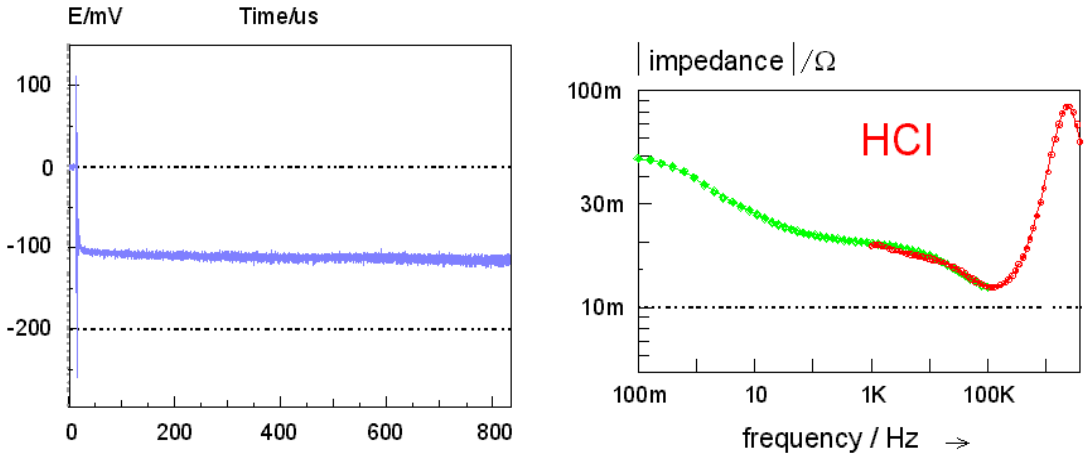


Fig. 12. Left hand side: HCI measurement of a single solid oxide fuel cell at 866°C and 4 A. Right hand side: Impedance (EIS) between 100 mHz – 100 kHz (green); frequency transformed HCI: 1 kHz – 800 kHz (red)

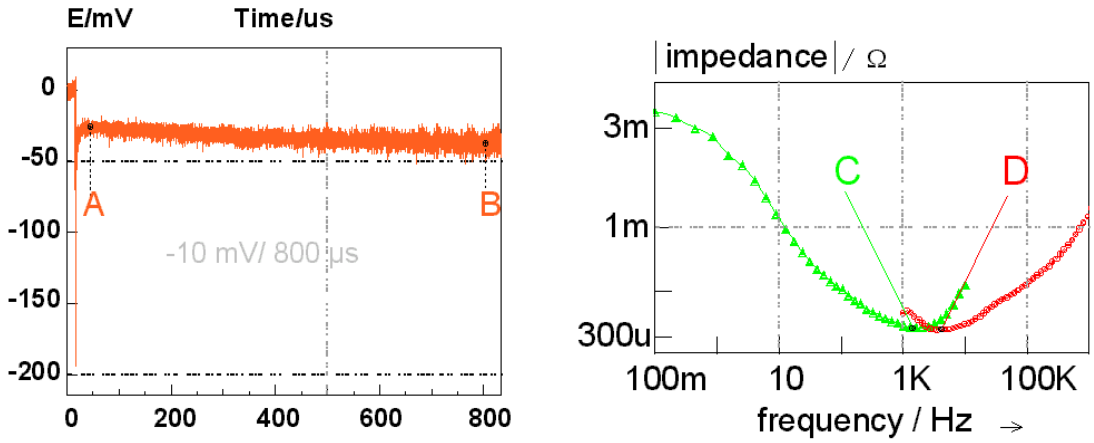


Fig. 13. HCI measurement of a single PEM fuel cell at 85° C and 80 A. Left: time domain data. Between time moments A and B the voltage changes for ≈10mV. Right: the resulting spectrum (squares, D) is compared with the result, achieved by standard EIS (triangles, C).

The last example demonstrates that the dominating error caused by the unavoidable mutual induction may falsify the result of standard EIS measurements in case of very

low impedance objects. In the experiments depicted in Fig. 13, a transformed HCI measurement is compared again with a standard EIS measurement.

The measurements were performed with a relatively large PEM fuel cell at a current of 80 A. The shift of the impedance minimum for the transformed HCI-data (circles) to higher frequencies indicates that the HCI measurement suffers less from the mutual induction compared to the EIS.

In the opinion of the authors, the lack of correspondence between the EIS- and the HCI-data at the low frequency end of 1.1 KHz results from a non-linear component in the long term pulse response signal: HCI analysis, like EIS, has to rely on the rule of linearity. The transient change of about -10 mV within the 0.85-milliseconds-analysis-interval may be enough to deviate from this rule.

2.1. Conclusions

1. EIS capabilities are basically limited by mutual induction in the high-frequency / low-impedance region. This falsifies significantly the results for Ohmic and inductive share.

2. The HCI capability is limited by the magnetic energy stored in the load circuit.

3. The HCI analysis can be automatically analyzed reliably by transforming the time data into the frequency domain.

4. According to the experience, HCI can extend the available frequency range with a factor of about three to ten in a carefully optimized experimental set-up.

5. HCI data interpretation should not be extended to the low frequency response. The unavoidable deviation from the EIS linearity rule after a certain interruption time may lead to misinterpretations.

6. Thus, an arrangement which performs both the standard EIS and the HCI measurement within one set-up, is the best choice for the challenges of electrochemical power source device testing

.

In a second example of a time domain technique, which supplements EIS, the Relaxation Voltammetry (RV) is presented.

3. RELAXATION VOLTAMMETRY (RV) - A METHOD FOR THE EVALUATION OF BARRIER COATINGS

Products, made of steel, have excellent mechanical properties. In addition, steel is an inexpensive material and therefore, iron in the form of steel is one of the most important technical raw materials of the daily life. Unfortunately, the chemical characteristics of steel are not so favourable. As a base metal, iron is sensitive to oxygen and humidity. As a consequence, unprotected steel corrodes very easily and the corrosion process affects not only the visual appearance but also influences the mechanical properties unfavourably.

One way to protect iron surface against corrosion is the application of organic coatings. The development of new coatings requires methods to optimize the formulation, which have to be tested during their development by the coatings manufacturers. To obtain a ranking of the corrosion protective performance of new coating formulations, many different weathering tests are necessary. After the weathering, the degradation of the coating has to be evaluated using mainly mechanical tests or visual examination. These tests are time consuming and the degree of degradation has to be estimated. The need of an objective and relatively fast evaluation method is obvious. Here, electrochemical impedance spectroscopy (EIS) is widely used for the characterization as well as for the detection of defects in the coating. Moreover, this method is also applied to determine of the water-uptake and the degree of blistering and delamination. EIS provides information about the mechanistic background of the corrosion processes as well as detailed information about coating properties like capacitance C_C or coating/pore resistance R_C.

For the interpretation of EIS-data, physical models like equivalent circuits are required. The basic models are given in Fig. 14. Model A describes a realistic perfect 'barrier coating' with the coating capacitance C_C and the coating/pore resistance R_C. Model B represents the case of pores and defects in the coating with a second 'time-constant', which correlates with the charge transfer, consisting of the charge transfer resistance R_{CT} and the double layer capacitor C_{DL}. This model is widely used in the literature.

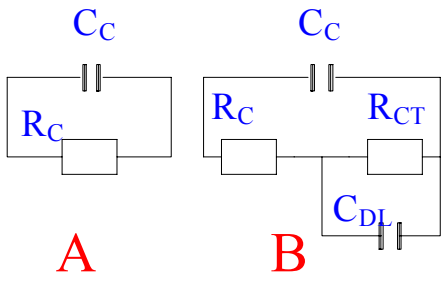


Fig. 14. Most popular basic equivalent circuits for the interpretation of EIS spectra of organic coatings.

Unfortunately, the application of EIS to corrosion research shows some handicaps. For instance, commercially available 'barrier coatings' often show a low-frequency resistance of the order 10^{10} $\Omega \cdot cm^{-2}$ or more. This requires a 'low frequency limit' of the measured spectrum in the mHz-region for the determination of R_C. Such measurements are rather time-consuming. Their duration can easily exceed one hour.

Next, the measured system has to be in a steady state during the whole measuring time interval. Concerning water-uptake measurements for instance, it is safe to assume that the constancy of the coating parameters (C_C and R_C) is not present in the early state of immersion. At least, considering the ratio of the number of measured specimens and the time, required for a single measurement, a single impedance measurement seems to be rather time expensive.

In contrast to measurements of barrier coatings in the frequency domain, traditional methods in the time domain suffer from the specific disadvantages of this kind of systems. For instance, static DC-measurements enable the determination of R_C, but they will not provide any information about dynamic parameters, neither about the dielectric

properties nor about 'dynamic' processes (like diffusion contributions) within the coating. The dynamic measurements in the time domain, which are reported in the literature [4,5], i. e. current interrupt techniques, suffer from the high resistances of the coating materials, too. On one hand, the so-called electrometers have an excellent accuracy in measuring current. Unfortunately, these electronic devices are showing a poor resolution in time[1]. Due to this fact, these instruments are not able to monitor (or to separate) fast processes. On the other hand, the current interrupt technique reported in the literature [5], delivers a resolution in measuring current of only 120 pA/digit. As it will be shown below, this resolution is by far too low.

A relatively new technique for the investigation of high-Ohmic systems is the *Relaxation Voltammetry* (RV) [6-9]. This method belongs to current interrupt technique too, but it was designed especially to overcome the problems noted above. The principle of this technique is depicted schematically in Fig. 15 and explained in the following.

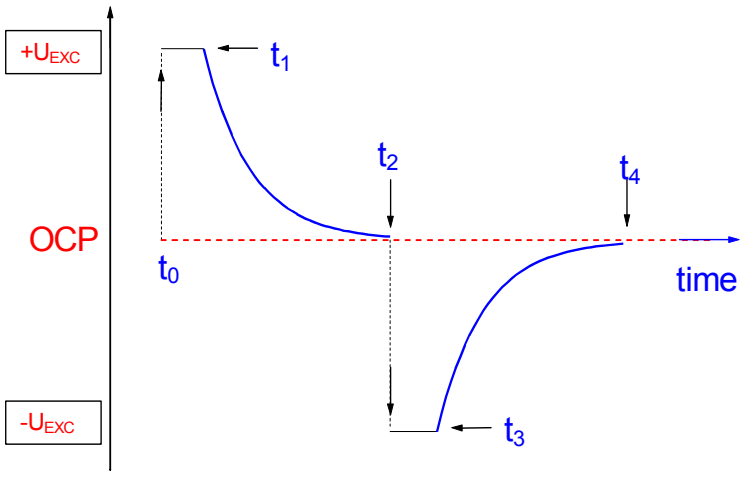


Fig. 15. The principle of Relaxation Voltammetry (RV)

The potential $+U_{EXC}$ is superimposed on the open circuit potential (OCP) and causes a transient current (I_{EXC}), which tends to be constant after a certain moment of time (t_1-t_0 = t_{EXC}). After the current reaches this stationary state, it is switched off and the following decay of the potential U(t) is recorded as a function of time (t_1 to t_2). The initial

[1] Usually, small currents are measured by integration of a voltage drop at a shunt-resistor. But, the smaller the current the longer the time of integration for a given accuracy. As a consequence, the sampling rate of an electrometer is less than one point per second at

stage of this relaxation process is monitored using a sampling rate of 600 points per second (about 40 to 100 data points) and then the sampling rate is lowered. After the potential reaches approximately the value of the OCP (at t_2 in Fig. 15), the procedure is repeated using the same potential but with the opposite sign ($-U_{EXC}$).

Taking into account the following considerations, the experimental procedure of RV differs essentially from 'traditional current interrupt techniques':

1.) In general, many electrochemical experiments are characterized by two parameters, potential and current. In potentiostatic mode of operation for instance, a potential is applied, whereas the corresponding quantity (the current) is measured as a function of the actual potential. In contrast, in RV experiment, a constant potential is applied and after interrupting the current, the potential is recorded as a function of the relaxation time. This kind of operation offers mainly two advantages. First of all, a potential in the range of 10^{-3} to 10^{-6} V can be measured more precisely than a current in the range of 10^{-12} to 10^{-15} A in principle. Secondly, the current ($\pm$) I_{EXC} is measured at its highest level, integrating over a small time interval (about five seconds) before the interruption occurs, improving the accuracy additionally.

2.) Anodic **and** cathodic excitations are performed and both transients are measured. For the evaluation of the transient response U(t), the values of both half-cycles are averaged, resulting in a 'symmetrical square-wave perturbation' around the OCP - similar to EIS.

3.) This 'symmetrical' operation is important, considering the experimental fact, obtained from measurements of barrier coatings, that the transients would not return exactly to the initial value of the OCP observed before the excitation. In a continuous mode of operation, t_{EXC} and/or U_{EXC} can be varied in subsequent cycles. Performing only anodic **or** cathodic excitation - like in 'traditional interrupt techniques' - would result in an irreversible shift[2] of the OCP. This would lead to erroneous results due to a superimposed (rest-) relaxation caused by the offset between the 'end-potential' (at t_2/t_4 in Fig. 15) and the OCP. To overcome this problem, in RV the

---

the pA–level [7].

[2] A similar effect which is commonly observed in water-uptake measurements, results from the drift of the OCP caused by the measured system itself.

OCP is ‘updated’ after each half-cycle from the values of the ‘end-potential’ of the actual and the latter half-cycle (for instance: OCP = ½ (U_{t4} + U_{t2}).

For sufficient accuracy the duration of excitation has to be chosen long enough to achieve settling. Fig.16 illustrates the influence of too short settling time on the voltage response. For a good compromise between time expense and available precision it is advisable to select the excitation time individually for a particular type of coating.

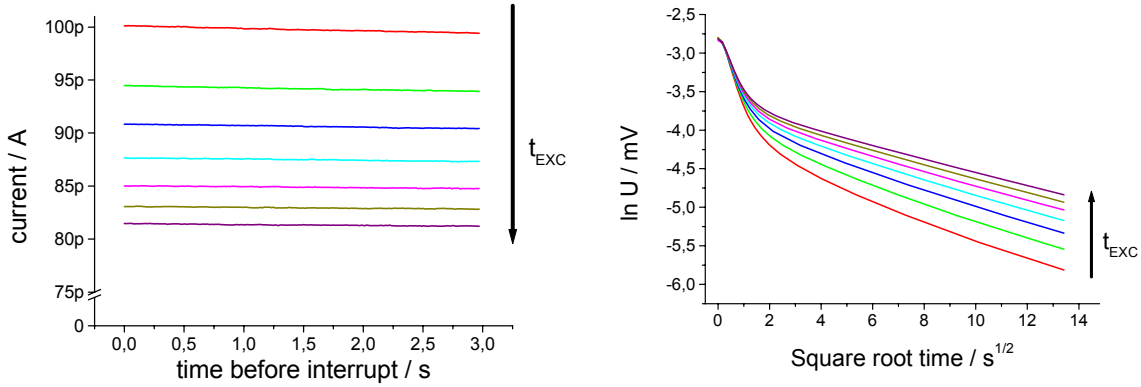


Fig. 16: Magnitude of the current before the interruption as a function of the excitation time t_{EXC} (left hand side) and the corresponding transients (right hand side). Scales are chosen for best visualization of the effect.

As one can see in Fig. 16 (left hand side), the current before the interruption decreases with increasing excitation time and settles at a constant value. The increased excitation time leads to a decrease in ‘speed’ of the corresponding transient, especially considering the long-time tail of the recorded voltage decay.

The applicability and performance of RV experiment can be best represented by an example and in comparison to a measurement using EIS. In Fig. 17, the result of an RV measurement of a barrier coating is plotted as a function of the square root of the relaxation time (right diagram) whereas an impedance spectrum of the same specimen is shown at the left hand side of Fig. 17.

The DC accuracy of RV experiment is best reflected regarding the small value of I_{EXC} ($1.33 \pm 0.01 \cdot 10^{-12}$ A), resulting from the total DC-resistance of the coating ($1.5 \cdot 10^{10}$ Ω

or $6.75 \cdot 10^{10}\ \Omega \cdot cm^{-2}$) [3]. The small diagram in the right part of Fig. 17 shows the initial voltage decay of the relaxation as a function of time. As it is indicated in the figure, the early state of the relaxation was measured with the higher sampling rate. The evaluation of this part of a RV-transient provides information about the dielectric properties of the system under investigation and therefore it gives an estimate of the dynamical performance of RV. This part will be discussed below in detail.

Comparing the results of EIS and RV experiments in Fig. 17, the complementary nature of both techniques becomes clear. Considering the time (frequency) scale of both methods, one has to conclude that EIS operates in the high frequency part (i.e. above 1 Hz) accurately and without consuming too much time for the measurement. But at lower frequencies, the measuring time interval increases drastically, which restricts the number of measured points (i. e. 5 points below 1 Hz in the above example) in practical measurements in a coating manufacturer's laboratory, which may result either in a loss of accuracy or of information.

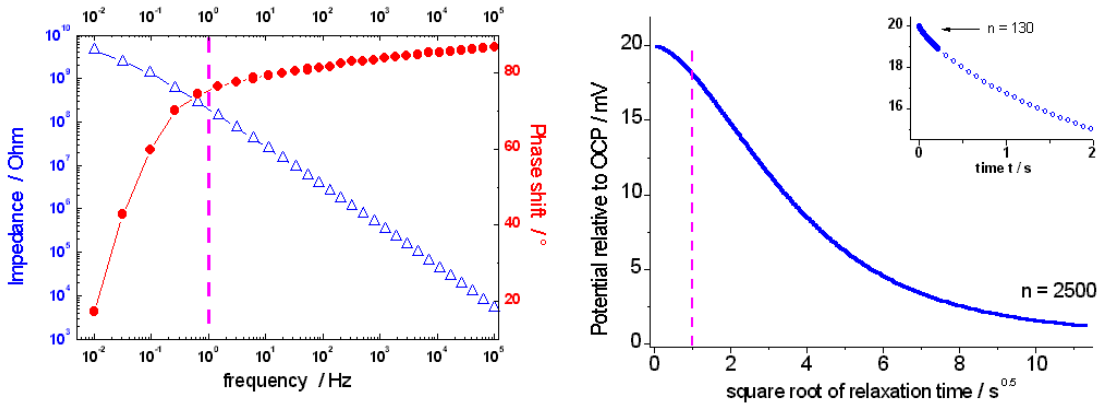


Fig.17. RV and EIS as complementary techniques

On the other hand, RV technique handles the middle and large relaxation range (above 1 second) which corresponds to the 'middle and low- frequency part' of an impedance spectrum very well. This fact is simply expressed by the number of measured points (n

[3] Measuring area : 4.5 cm^2

> 2000 above 1 second). A sufficient 'overlap' between the time scale of both methods arises from the initial sampling rate of RV, which is shown in the following.

3.1. The "dynamic" performance of RV

As it was noted above, the total DC-resistance R_T can be calculated immediately from the applied potential ($\pm U_{EXC}$) and the current ($\pm I_{EXC}$) before the interruption. In addition, RV delivers the coating capacitance C_C without the need of a detailed interpretation of the overall relaxation process.

Adopting the models for the interpretation of EIS-data (Fig. 14), this parameter is accessible from the initial slope (ISL) of the potential decay and I_{EXC} (scheme 1). From a theoretical point of view, the determination of C_C based on the ISL is exact for model A (Fig. 14) and an excellent approximation in the case of model B[4]. If necessary, the applicability of the ISL approach can be extended mathematically, involving the quadratic term of the underlying power series (ISL_{EXC}).

$$U(t) = I_{EXC} R_T \cdot e^{-\frac{t}{R_T C_C}} = I_{EXC} R_T - \frac{I_{EXC}}{C_C} t + \frac{I_{EXC}}{2 \cdot R_T \cdot C_C^2} t^2 \pm \ldots$$

$$ISL = \lim_{t \to 0} \frac{dU}{dt} = -\frac{I_{EXC}}{C_C}$$

$$ISL_{EX} = \lim_{t \to 0} \frac{dU}{dt} = -\frac{I_{EXC}}{C_C} + \frac{I_{EXC}}{2 \cdot C_C{}^2 \cdot R_T}$$

Scheme 1: The initial slope approximation (ISL)

From a practical point of view, the scope and accuracy of the ISL approximation has been first verified by measurements with equivalent circuits. From the results of these measurements [6-9] the accuracy of determination of C_C is about 10% or better for typical values, which are observed when measuring coating materials, i. e. capacitors in the range of ≥100 pF and total DC-resistances of ≥50 MΩ, respectively. Two examples for the determination of C_C' using the ISL approximation are depicted in Fig. 18.

In the upper part of the diagram an equivalent circuit (model B) with a total resistance R_T of 305 MΩ and a 'coating capacitance' of 150 pF is shown. From the voltage decay (≈ 2mV) during the first 4 milliseconds, an initial slope of -630 mV/s can be evaluated. Considering the current I_{EXC} (98.4 pA) yields a coating capacitance of 158 pF. In the second example an equivalent circuit (model B) with a total resistance R_T of 18.7 GΩ and a coating capacitance of 330 pF was used. The potential decay (≈ 200 µV) during the first 60 milliseconds gives an initial slope of -3.3 mV/s. With the current I_{EXC} (1.1 pA) a coating capacitance of 333 pF was calculated. This example additionally demonstrates that noise effects play an insignificant role at this early stage of the relaxation. In both cases an excellent agreement between theoretical results and experimental data is observed.

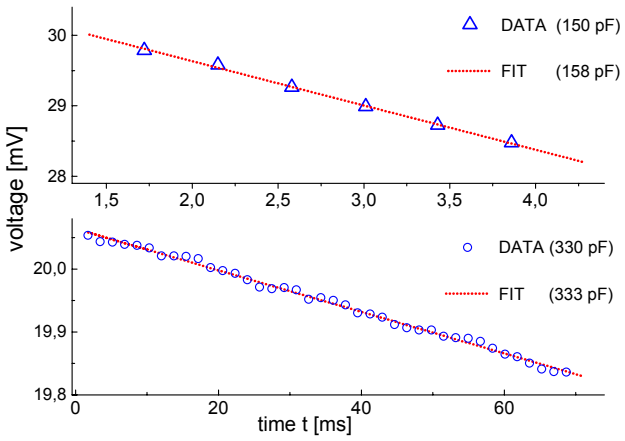


Fig. 18. ISL of two dummy cells (model B)

Fig. 19 shows a typical example of the evaluation of C_c of coatings using the ISL method. The voltage drop (squares) during the first 10 milliseconds is about 500 µV. Comparing the starting potential decay with the values obtained from dummy measurements it becomes evident that the linear range turns out to be much shorter than predicted based on the models given in Fig. 14. The deviation from linearity (triangles = ISL) occurs already below 4 milliseconds. Therefore, to evaluate the coating capacitance the extended ISL_{EX} (circles) was used. The analysis of the linear part gives an initial potential decay of -53 mV/s, yielding a coating capacitance of 250 pF.

[4] The physical background of this approximation is that the current through the capacitor C_{DL} can be neglected at the initial stage of

Further applications of RV experiment in corrosion research of coated metals are reported in more detail in the literature [7, 10-12].

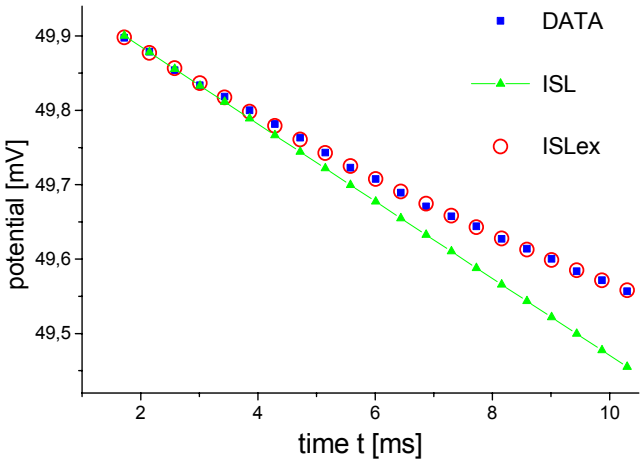


Fig. 19. Typical ISL of a coating

In a comprehensive analysis of a huge number of different coating materials over a wide range of relaxation times it was found out that the dielectric relaxation in barrier coatings can be explained by a hopping (random walk) process [13]. It is noteworthy that this so-called 'two-step continuous time random walk' (CTRW-2) exhibits a square root of time dependence of the corresponding time-law (equation 3), which seemed to contradict the results of EIS (see also [14,15]).

$$\phi(t) = \frac{U(t)}{U_{EXC}} = \frac{1}{4^{\beta}-1}\cdot\left\{4^{\beta}\cdot\exp\left[-(\lambda\cdot t)^{\beta}\right] - \exp\left[-(4\cdot\lambda\cdot t)^{\beta}\right]\right\}$$
$$with \quad 0 < \beta \leq 0.5 \quad and \quad \beta_{ideal} = 0.5 \qquad (3)$$

However, in two publications [16,17], it was proven that there is no contradiction between the interpretation of the results of both techniques in principle, concerning the evaluated dielectric parameters.

Moreover, the evaluation of experimental data in frequency- and time-domains according to the CTRW-2 process is now implemented into a commercially available software package. For this purpose two procedures have to be involved. On one hand, time domain data have to be transformed into the frequency domain to evaluate the RV data

---

the relaxation and therefore, model B in Fig. 1 reduces to model A.

with the techniques of EIS. The frequency transform is accomplished by a special kind of the discrete Fourier transform “Zoom Fast Fourier Transform“(ZFFT). A typical example is depicted in Fig. 20.

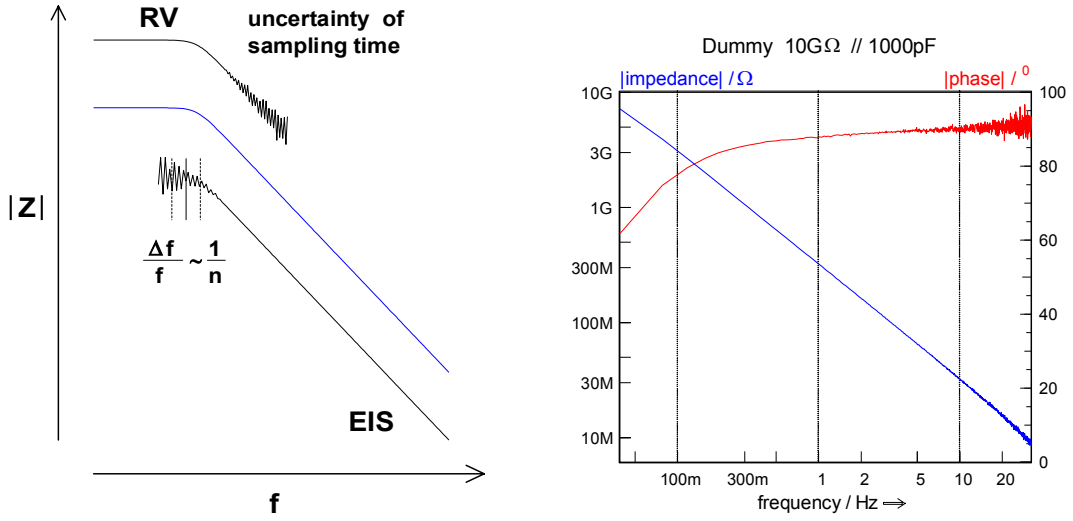


Fig. 20. Left hand side: ‘complementary properties’ of EIS and transformed RV data. Typical result of a frequency transformed RV transient (right hand side)

On the other hand, a numerical representation of the CTRW-2 process has been established to evaluate impedance data in the frequency domain according to this model. As it was noted above, the processing of experimental data in the frequency domain benefits due to more simple mathematical operations provided the transfer function of a distinct impedance element is known. Unfortunately, a definite analytical expression of the CTRW-2-function in the frequency domain does not exist. The transformation presented in the literature is a combination of numerical and analytical algorithms, designed for the evaluation of a sufficiently wide range of frequencies, which is convenient for the user. Further details are reported in the literature [18].

3.2. Conclusions

It has been shown that RV experiment is a suitable tool for the investigation of high impedance systems. Although different applications can be seen, RV technique has been especially designed to meet the demands of the investigation of coated metals.

In contrast to 'traditional interrupt techniques', RV experiment combines electrometer-type accuracy with an adequate resolution in time so that DC- as well as dielectric parameters of these systems are accessible. Both quantities are of great importance for the coatings manufacturer to improve their products. In comparison to EIS it is to claim that both techniques supplement each other ideally. Undoubtedly, the big advantage of EIS for the evaluation of high impedance systems is the rapid determination of the dielectric properties, whereas the strong advantages of RV method are found to be in the 'middle and low frequency range'. At last, the RV equipment is less expensive so that several measurements can be performed in parallel. This reduces the time consumption in the manufacturer's laboratory additionally.

4. REFERENCES

1. C. A. Schiller, in: "Introduction to Electrochemical Instrumentation", "Analytical Methods in Corrosion Science and Engineering", P. Marcus and F. Mansfeld (eds.); Taylor & Francis, Boca Raton, 2005.
2. D. E. Vladikova, Z. B. Stoynov, G. S. Raikova, in: "Inductance Error Correction in Impedance Studies of Energy Sources", "Portable and Emergency Energy Sources", Z. Stoynov, D. Vladikova, (eds.), Prof. Marin Drinov Academic Publishing House, Sofia, 2006.
3. W. Ehm, R. Kaus, C. A. Schiller, W. Strunz, in: "New Trends in Electrochemical Impedance Spectroscopy and Electrochemical Noise Analysis", F. Mansfeld, F. Huet, O. R. Mattos (eds.), Electrochemical Society Inc., Pennington, NJ, 2001, vol. 2000-24, 1.
4. R. D. Granata, K. J. Kovaleski, in: "Evaluation of High- Performance Protective Coatings by Electrochemical Impedance and Chronoamperometry", "Electrochemical Impedance: Analysis and Interpretation", J. R. Scully, D. C. Silverman, M. W. Kendig (eds.), ASTM STP, 1993, p.1188.
5. H. Tanabe, M. Nagai, H. Matsuno, M. Kano, in: "Evaluation of protective coatings by a current interrupter technique" in "Advances in Corrosion Protection by Organic Coatings II" (1994); ISBN 1-56677-108-0; pages 181 – 192; (from: Materials and Corrosion 47 (1996), abstract Nr. 96-0831).

6. G. Meyer, H. Ochs, W. Strunz, J. Vogelsang, in: “Barrier coatings with high Ohmic resistance - comparison between Relaxation Voltammetry and Impedance Spectroscopy”, Proceed. EMCR 1997, 25–29.8.1997, Trento, Italy, oral contribution.
7. G. Meyer, H. Ochs, W. Strunz, J. Vogelsang, Materials Science Forum 289 (1998) 305.
8. H. Ochs, W. Strunz, J. Vogelsang, in: “Relaxation voltammetry with organic barrier coatings on steel - experimental and theoretical approach”, Proceed. EMCR 1997, 25–29.8.1997, Trento, Italy, poster presentation.
9. G. Meyer, H. Ochs, W. Strunz, J. Vogelsang, Materials Science Forum 289 (1998) 373.
10. W. Strunz, J. Vogelsang, in: “Characterization and evaluation of organic coatings using relaxation voltammetry”, Proceed. EUROCORR 1998, Utrecht, Netherlands, oral contribution.
11. J. Vogelsang, W. Strunz, in: “Barrier coatings - a challenge for EIS and RV”, Proceed. EIS 1998, Rio de Janeiro, Brasil.
12. J. Vogelsang, U. Eschmann; G. Meyer, W. Strunz, Farbe & Lack 104:5 (1998) 28.
13. W. Strunz, Prog. Org. Coat. 39 (2000) 49.
14. J. Vogelsang, W. Strunz, Materials and Corrosion 52:6 (2000) 462.
15. J. Vogelsang, W. Strunz, Electrochim. Acta 46 (2001) 3817.
16. C. A. Schiller, W. Strunz, Electrochim. Acta 46 (2001) 3619.
17. W. Strunz, in: “*The frequency behavior of the “two-step” continuous time random walk”*, Proceed. EMCR 2000, Budapest, Hungary, oral contribution.
18. W. Strunz, C. A. Schiller, J. Vogelsang, Electrochim. Acta 51 (2006) 1437.